Supporting Information

Gamze Gezer,[a] Dinesh Durán Jiménez,[a] Maxime A. Siegler,[b] and Elisabeth Bouwman*,[a]

[1] *Leiden Institute of Chemistry, Leiden University, P.O. Box 9502, 2300 RA Leiden, the Netherlands*

[b] *Department of Chemistry, Johns Hopkins University, 21213 Maryland, U.S.A*

E-mail: bouwman@chem.leidenuniv.nl

Table of Contents

Table S1: Crystal and structure refinement data for complexes **(3)**, **(5)** and **(6)**

Experiments were carried out at 110 K using a SuperNova, Dual, Cu at zero, Atlas. H-atom parameters were constrained.

	(3)	**(5)**	**(6)**
Crystal data			
Chemical formula	$C_{11}H_{22}NiS_2Se_2$	$C_{17}H_{27}FeNiOS_2Se_2 \cdot F_6P$	$C_{22}H_{29}FeNiOS_2Se_2 \cdot F_6P \cdot CH_2Cl_2$
M_r	435.03	728.95	875.95
Crystal system, space group	Monoclinic, $P2_1$	Trigonal, R-3:H	Monoclinic, $P2_1/c$
a, b, c (Å)	7.2301 (2), 10.3586 (2), 10.5707 (3)	31.5009 (7), 31.5009 (7), 14.4145 (4)	10.32665 (13), 22.8030 (2), 13.72057 (17)
α, β, γ (°)	90, 103.465 (3), 90	90, 90, 120	90, 105.9916 (13), 90
V (Å^3)	769.92 (4)	12387.3 (6)	3105.87 (6)
Z	2	18	4
Radiation type	Mo $K\alpha$	Cu $K\alpha$	Cu $K\alpha$
μ (mm^{-1})	6.23	10.52	11.00
Crystal size (mm)	0.26 × 0.19 × 0.03	0.18 × 0.05 × 0.04	0.36 × 0.08 × 0.04
Data collection			
Absorption correction	Analytical *CrysAlis PRO*, Agilent Technologies, Version 1.171.36.32 (release 02-08-2013 CrysAlis171 .NET) (compiled Aug 2 2013,16:46:58) Analytical numeric absorption correction using a multifaceted crystal model based on expressions derived by R.C. Clark & J.S. Reid. (Clark, R. C. & Reid, J. S. (1995). Acta Cryst. A51, 887-897)	Gaussian *CrysAlis PRO*, Agilent Technologies, Version 1.171.36.32 (release 02-08-2013 CrysAlis171 .NET) (compiled Aug 2 2013,16:46:58) Numerical absorption correction based on gaussian integration over a multifaceted crystal model	Analytical *CrysAlis PRO*, Agilent Technologies, Version 1.171.36.32 (release 02-08-2013 CrysAlis171 .NET) (compiled Aug 2 2013,16:46:58) Analytical numeric absorption correction using a multifaceted crystal model based on expressions derived by R.C. Clark & J.S. Reid. (Clark, R. C. & Reid, J. S. (1995). Acta Cryst. A51, 887-897)
T_{min}, T_{max}	0.316, 0.839	0.414, 0.788	0.161, 0.716
No. of measured, independent and observed [$I > 2\sigma(I)$] reflections	11826, 3544, 3416	16503, 5401, 4525	20451, 6094, 5655
R_{int}	0.030	0.032	0.033
$(\sin \theta/\lambda)_{max}$ (Å^{-1})	0.649	0.616	0.616
Refinement			

$R[F^2 > 2\sigma(F^2)]$, $wR(F^2)$, S	0.022, 0.050, 1.04	0.039, 0.084, 1.06	0.030, 0.077, 1.03
No. of reflections	3544	5401	6094
No. of parameters	149	284	405
No. of restraints	1	0	181
	$w = 1/[\sigma^2(F_o^2) + (0.0249P)^2 + 0.0526P]$ where $P = (F_o^2 + 2F_c^2)/3$	$w = 1/[\sigma^2(F_o^2) + (0.0255P)^2 + 67.0697P]$ where $P = (F_o^2 + 2F_c^2)/3$	$w = 1/[\sigma^2(F_o^2) + (0.0416P)^2 + 2.5519P]$ where $P = (F_o^2 + 2F_c^2)/3$
Δ_{max}, $\Delta\rangle_{min}$ (e Å^{-3})	0.47, -0.33	0.47, -0.92	0.90, -0.89
Absolute structure	Flack x determined using 1521 quotients [(I+)-(I-)]/[(I+)+(I-)] (Parsons, Flack and Wagner, Acta Cryst. B69 (2013) 249-259).	–	–
Absolute structure parameter	0.002 (5)	–	–

Computer programs: *CrysAlis PRO*, Agilent Technologies, Version 1.171.36.32 (release 02-08-2013 CrysAlis171 .NET) (compiled Aug 2 2013, 16:46:58), *SHELXS2014*/7 (Sheldrick, 2015), *SHELXS2014*/7 (Sheldrick, 2014), *SHELXL2014*/7 (Sheldrick, 2015), *SHELXL2014*/7 (Sheldrick, 2014), *SHELXTL* v6.10 (Sheldrick, 2008).

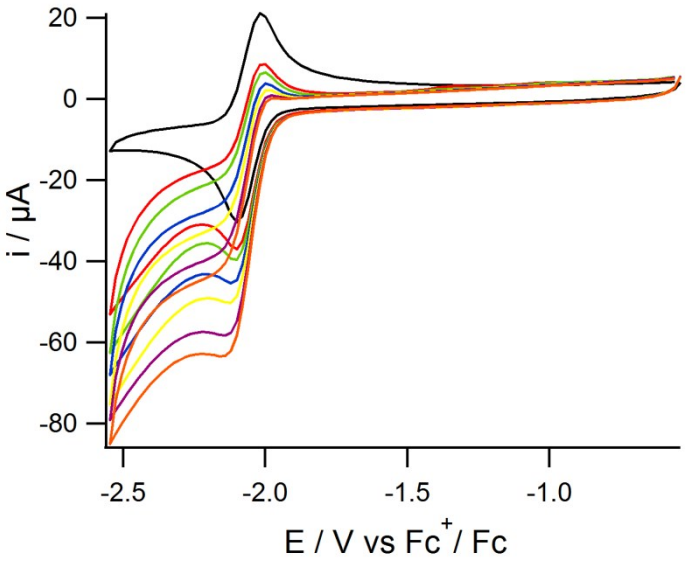

Figure S1**:** Cyclic voltammogram of [Ni(pbSmSe)] **(3)** in a DMF solution of $TBAPF_6$ (0.1 M) on a glassy carbon electrode at 200 mV s^{-1} with 0 (black), 10 (red), 20 (green), 30 (blue), 40 (yellow), 50 (purple), 60 (orange) mM of acetic acid.

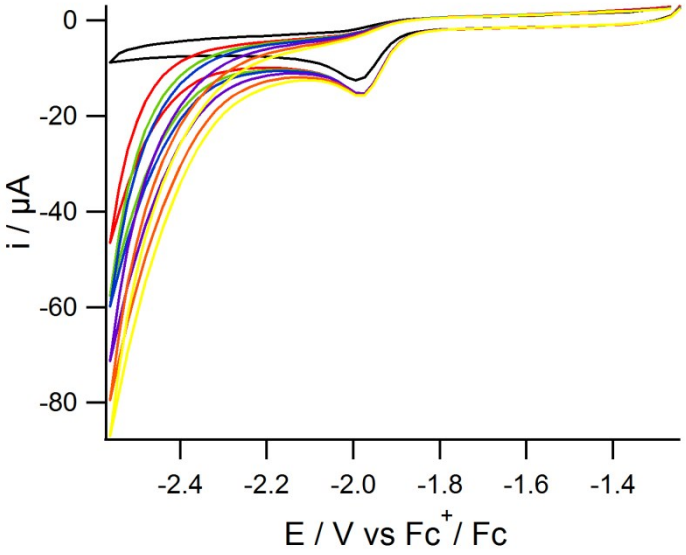

Figure S2**:** Cyclic voltammogram of [Ni(xbSmSe)] **(4)** in a DMF solution of $TBAPF_6$ (0.1 M) on a glassy carbon electrode at 200 mV s^{-1} with 0 (black), 10 (red), 20 (green), 30 (blue), 40 (yellow), 50 (purple), 60 (orange) mM of acetic acid.

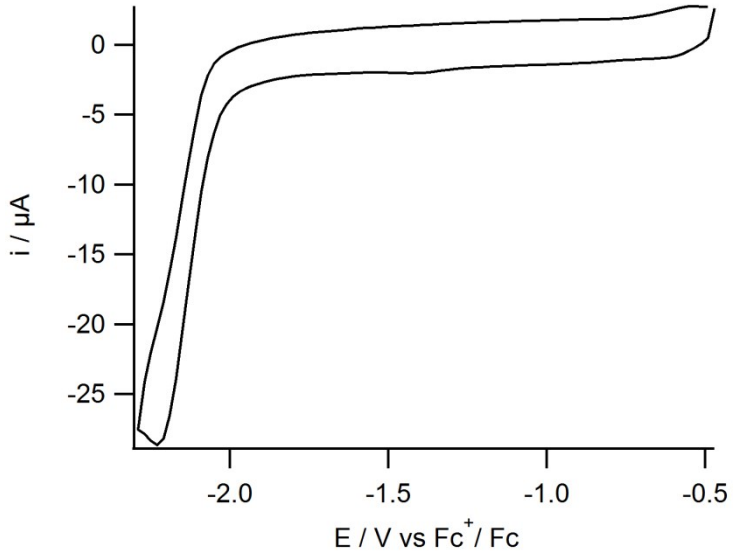

Figure S3**:** Cyclic voltammogram of [Ni(pbSmSe)] **(3)** in a DCM solution of $TBAPF_6$ (0.1 M) on a glassy carbon electrode at 200 mV s^{-1}.

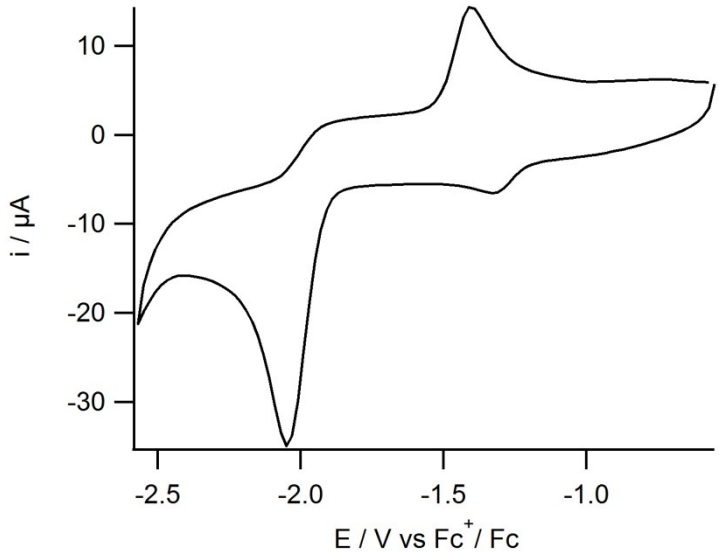

Figure S4**:** Cyclic voltammogram of $[FeCp(CO)_2I]$ in a DMF solution of $TBAPF_6$ (0.1 M) on a glassy carbon electrode at 200 mV s^{-1}.

Foot-of-the Wave Analysis

CV results were analyzed by using *FOWA* which helps to quantify the rates of HER. The observable rate constant (k_{obs}) can be obtained by plotting i/i_p^0 *vs* 1/1+exp[(F/RT)(E-E^0)] which gives a linear function at a certain scan rate. [1,2] For the complex **(5),** which has diffusion controlled reversible reaction, the current peaks (i and i_p^0) can be calculated according to equation (1) and (2): [1,2]

$$i_p^0 = 0.4463 F S C_p^0 \sqrt{\frac{FvD}{RT}} \qquad (1)$$

$$i = \frac{2FSC_p^0\sqrt{\frac{FvD}{RT}}}{1 + exp[\frac{F}{RT}(E - E^0)} \qquad (2)$$

where i_p^0 =90.17 µA, F is the Faraday's constant, S the surface of electrode, C_p^0 the concentration of the complex in solution, D the diffusion coefficient, E^0 the half-wave potential of the redox couple triggering catalysis, R the gas constant and T the temperature. Combining equation (1) and (2) gives us equation (3) which shows us plotting i/i_p^0 *vs* 1/1+exp[(F/RT)(E-E^0)] gives access of the observed rate constant (k_{obs}).

$$\frac{i}{i_p^0} = \frac{\frac{2}{0.4463}\sqrt{\frac{RT(k_{obs})}{Fv}}}{1 + exp[\frac{F}{RT}(E - E^0)]} \qquad (3)$$

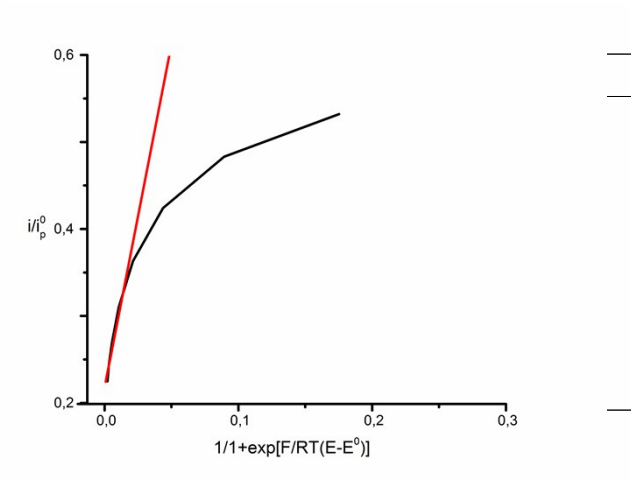

i (µA)	i / i_p^0	1/1+exp[F/RT(E–E^0)]
20.25	0.225	9.022x10^{-4}
21.93	0.243	1.964x10^{-3}
24.38	0.270	4.269x10^{-3}
27.95	0.310	9.256x10^{-3}
32.74	0.363	0.01995
38.23	0.424	0.04247
43.53	0.483	0.0881
48.01	0.532	0.174

Figure S5**:** Plot of i/i$_p^0$ vs. 1/1+exp[F/RT(E−E^0)] using FOWA of the complex **(5)** for H_2 evolution at 200 mV s^{-1} and a concentration of HOAc of 60 mM. The experimental data (black) can be fitted linearly near the foot of the catalytic wave and the slope (red) gives the access to the observed rate constant k_{obs}= k x C_A^0 according to equation (4). [2] Equation (5) [2] gives us access to k which is 402 M^{-1}s^{-1} and k_{obs} is 24 s^{-1}.

$$slope = \frac{2}{0.4463}\sqrt{(k_{obs})\frac{RT}{Fv}} \qquad (4)$$

$$k = \frac{slope^2 (0.4463)^2 Fv}{4RTC_A^0} \quad (5)$$

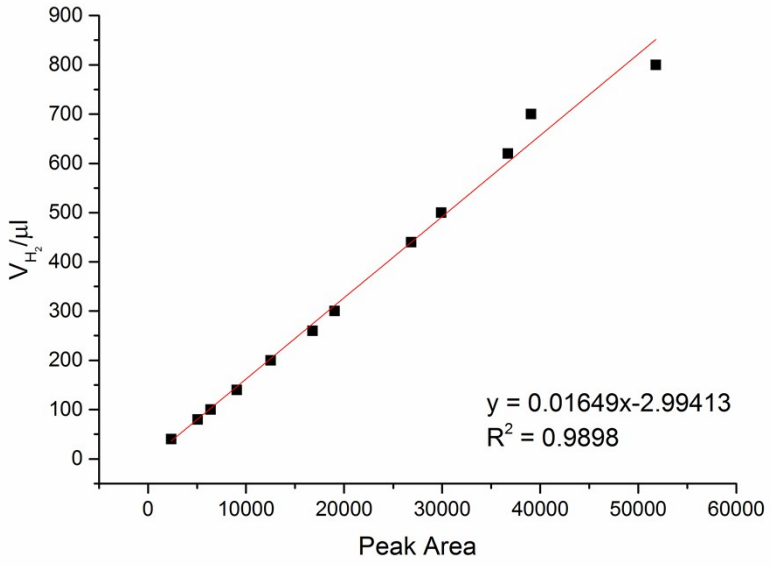

Figure S6**:** Calibration line used for CPC experiments. The observed peak areas of the GC are plotted against the volume of H_2 in the sample with an R^2 value of 0.9898.

Calculations are based on a calibration line obtained by the external reference method by injection of known amounts of H_2 into the system (Fig.S5). During the CPC experiment hydrogen is only produced from the local concentration of catalyst at the electrode surface. For this measurement, a glassy carbon electrode with 3 mm diameter was used. After 50 min the area of the H_2 peak is 4054 for the complex **(5)** and according to the equation from calibration line (Fig.S5):

$y = (0.01649 \times 4054) - 2.99413 = 64$ µl H_2

$(64 \times 10^{-6}) \div (24.465) = 2.6$ µmol H_2

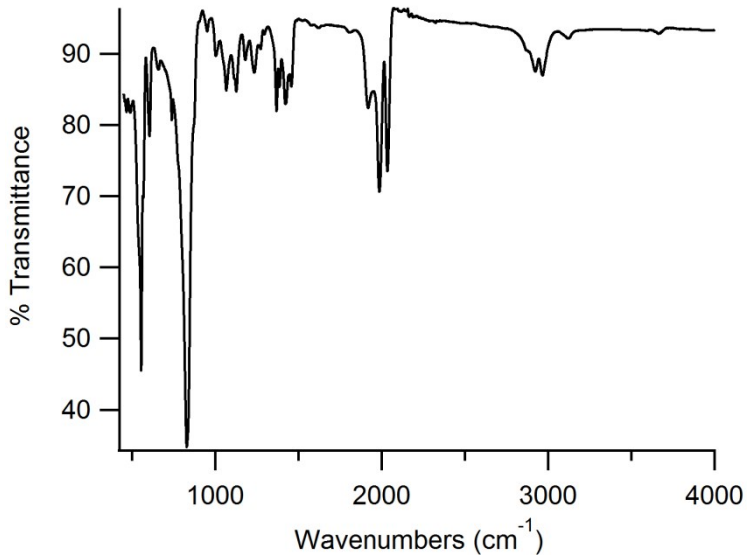

Figure S7**:** FTIR spectrum of the complex **(5)**.

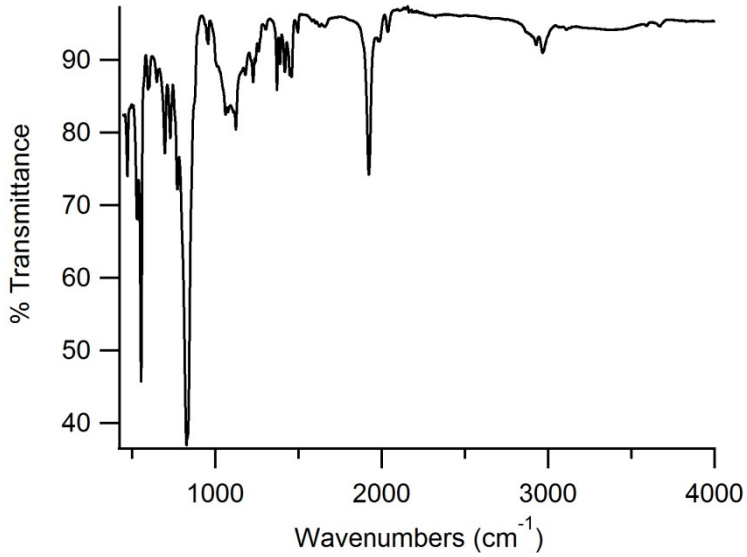

Figure S8**:** FTIR spectrum of the complex **(6)**.

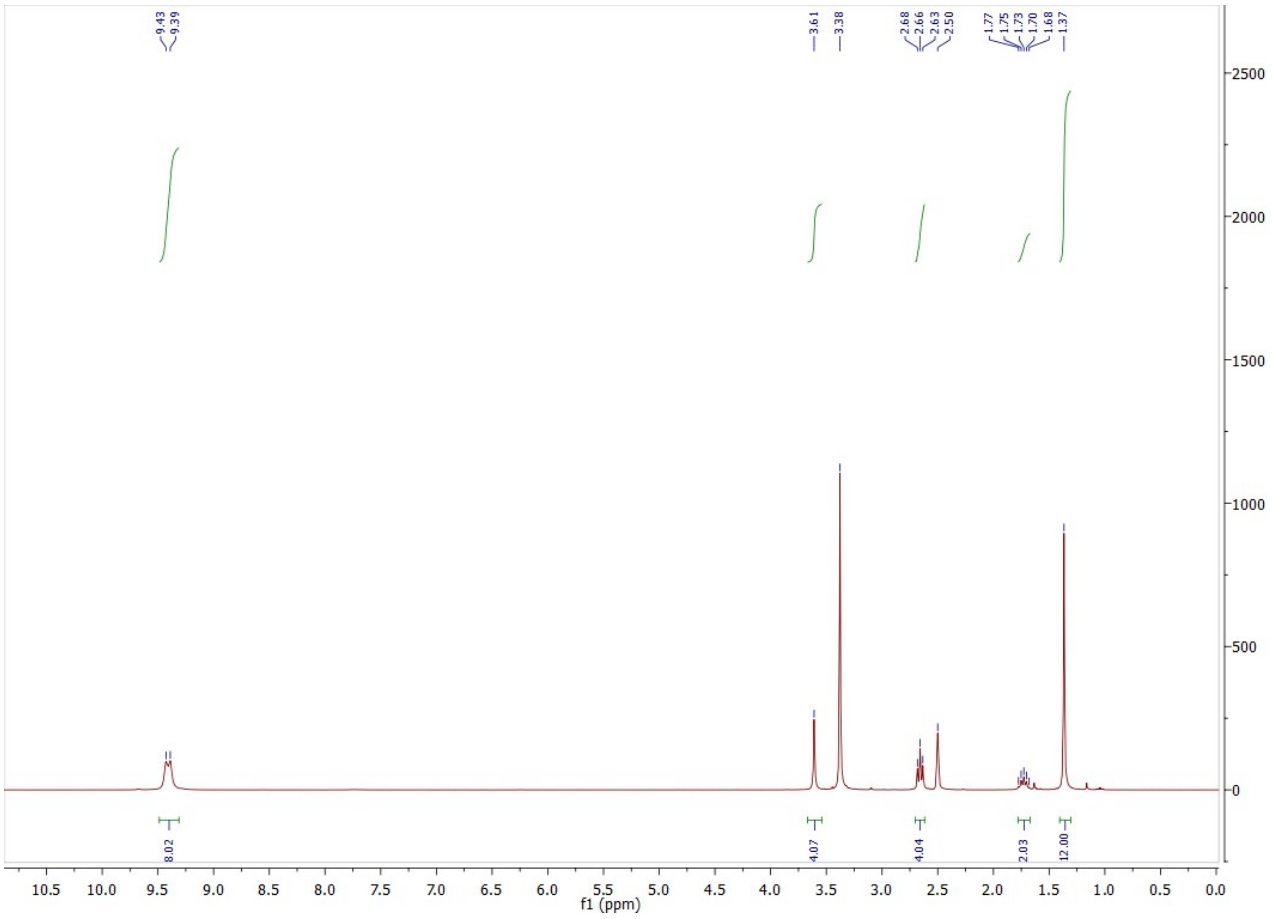

Figure S9: ^{1}H NMR spectrum of the ligand precursor **(1)** in DMSO.

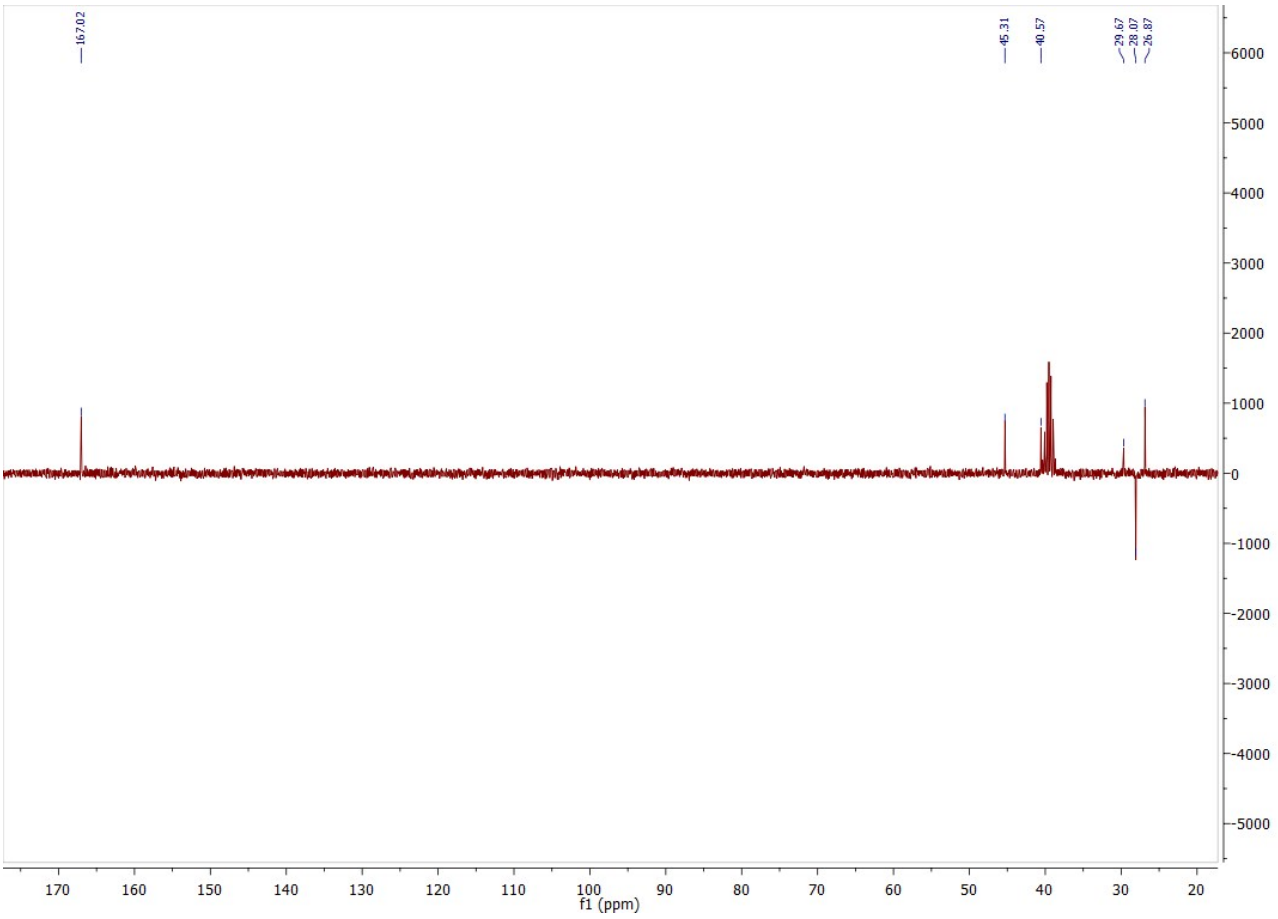

Figure S10: ^{13}C NMR spectrum of the ligand precursor **(1)** in DMSO.

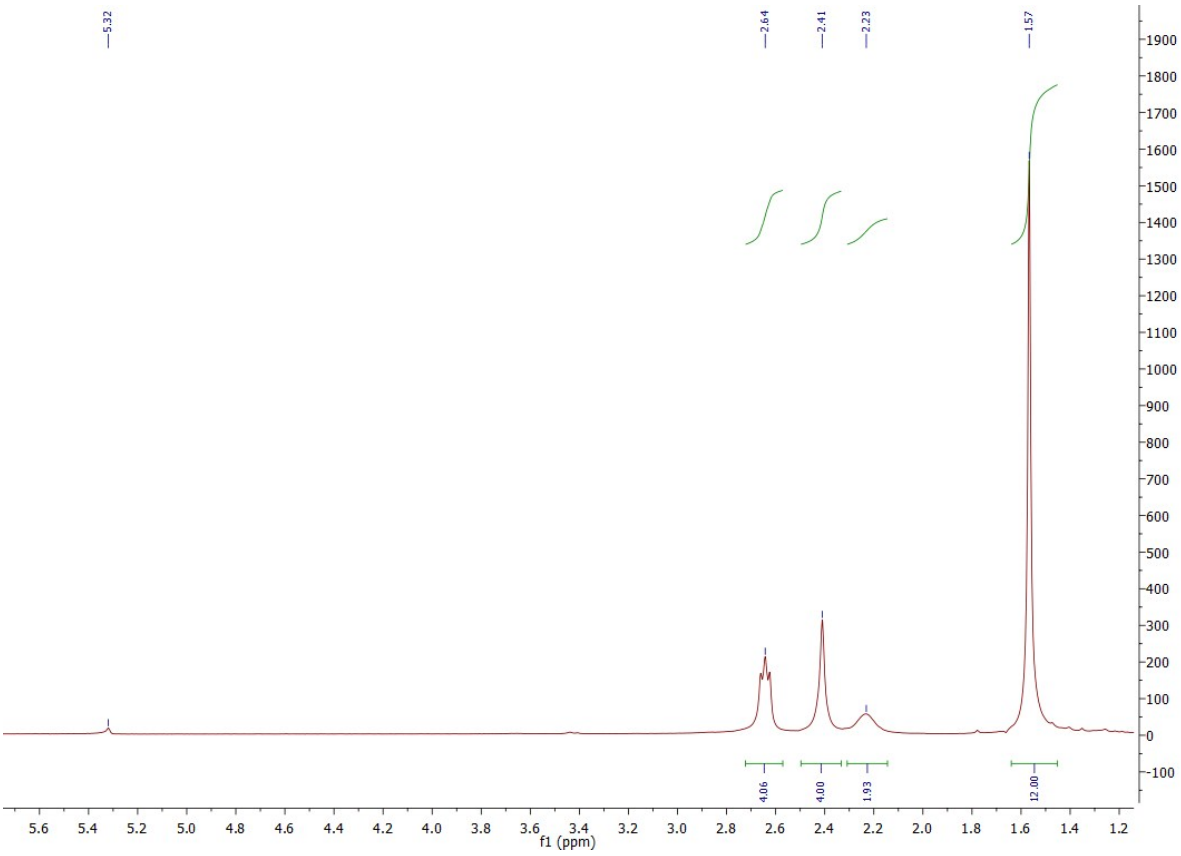

Figure S11: ^{1}H NMR spectrum of the complex **(3)** in DCM.

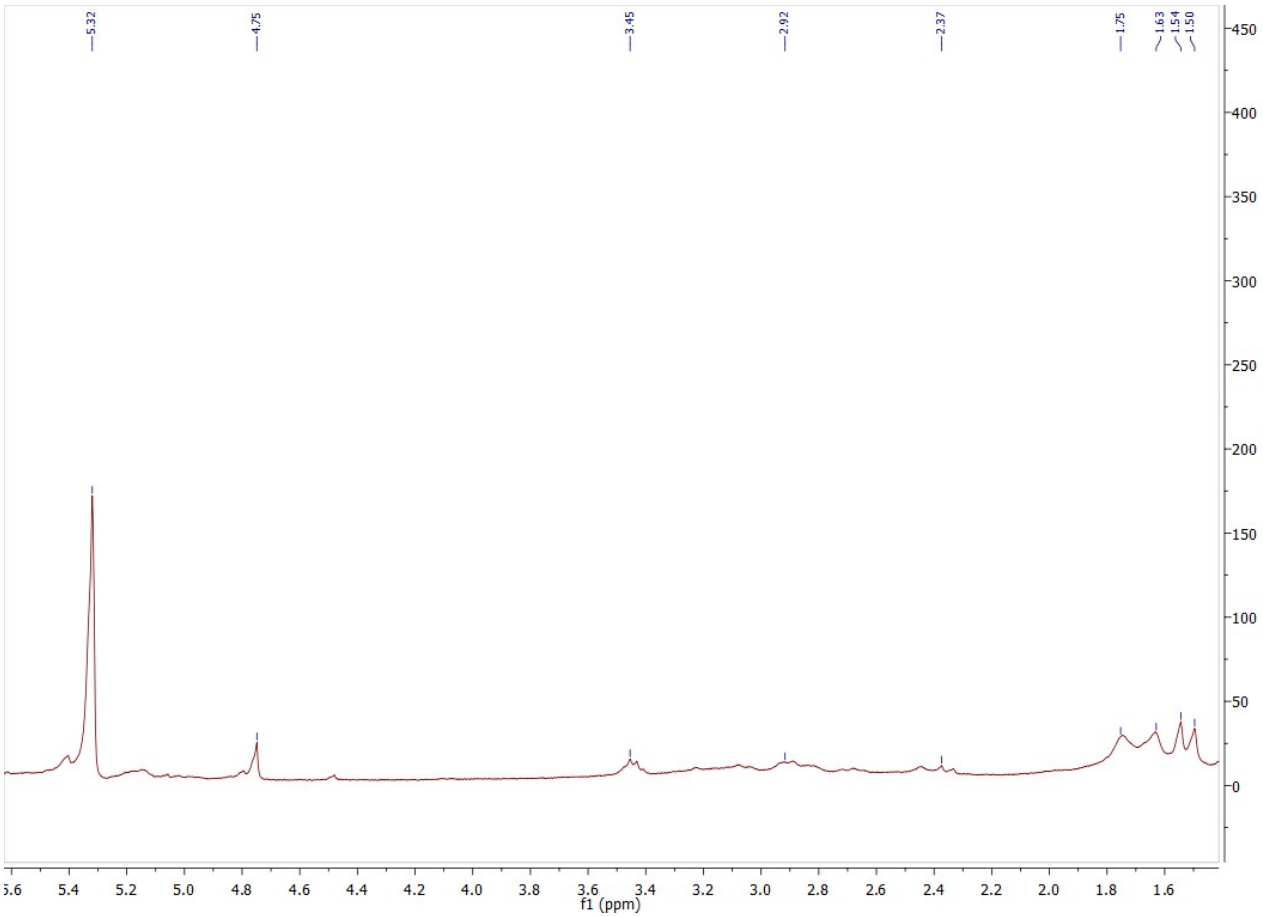

Figure S12: ^{1}H NMR spectrum of the complex **(5)** in DCM.

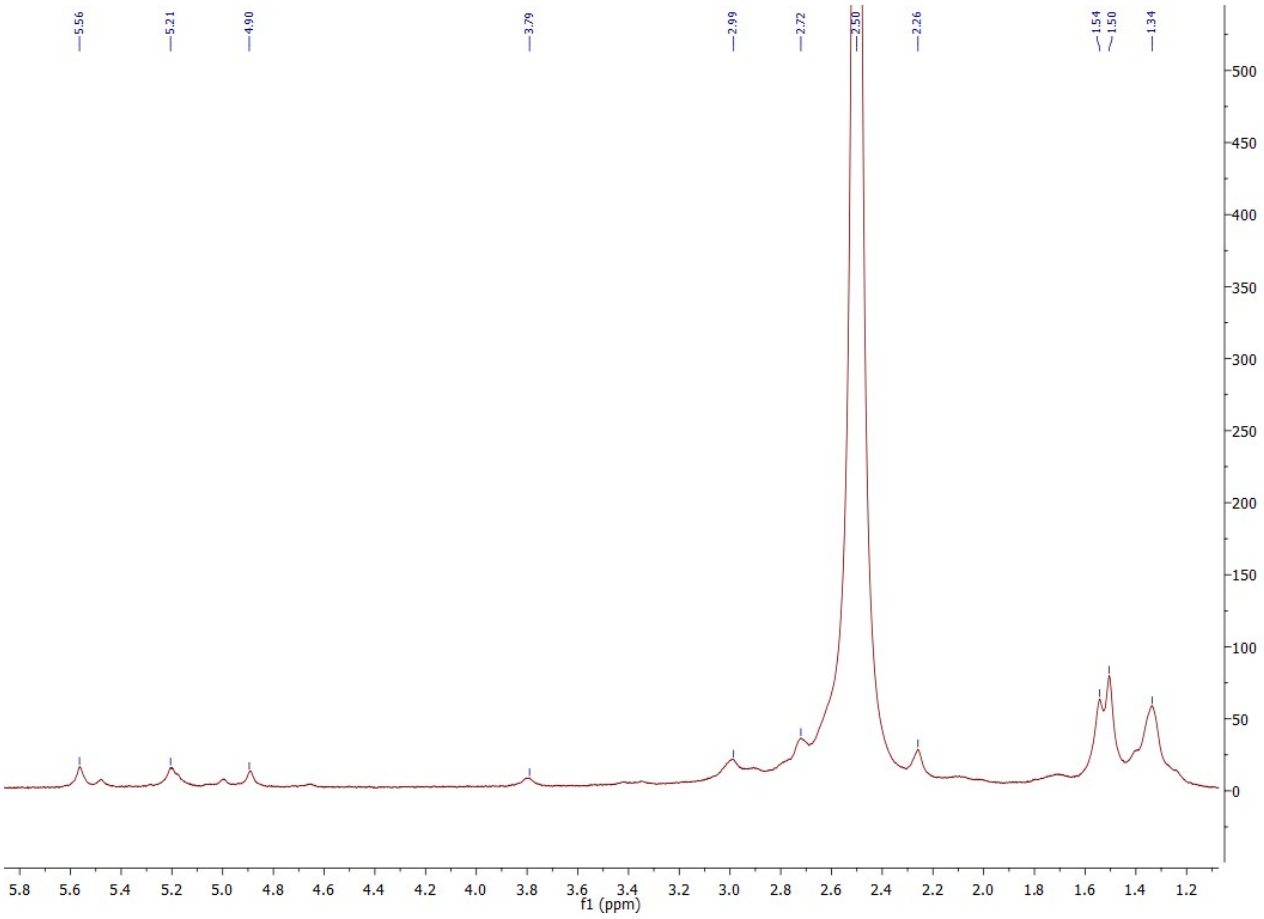

Figure S13: ^{1}H NMR spectrum of the complex **(5)** in DMSO.

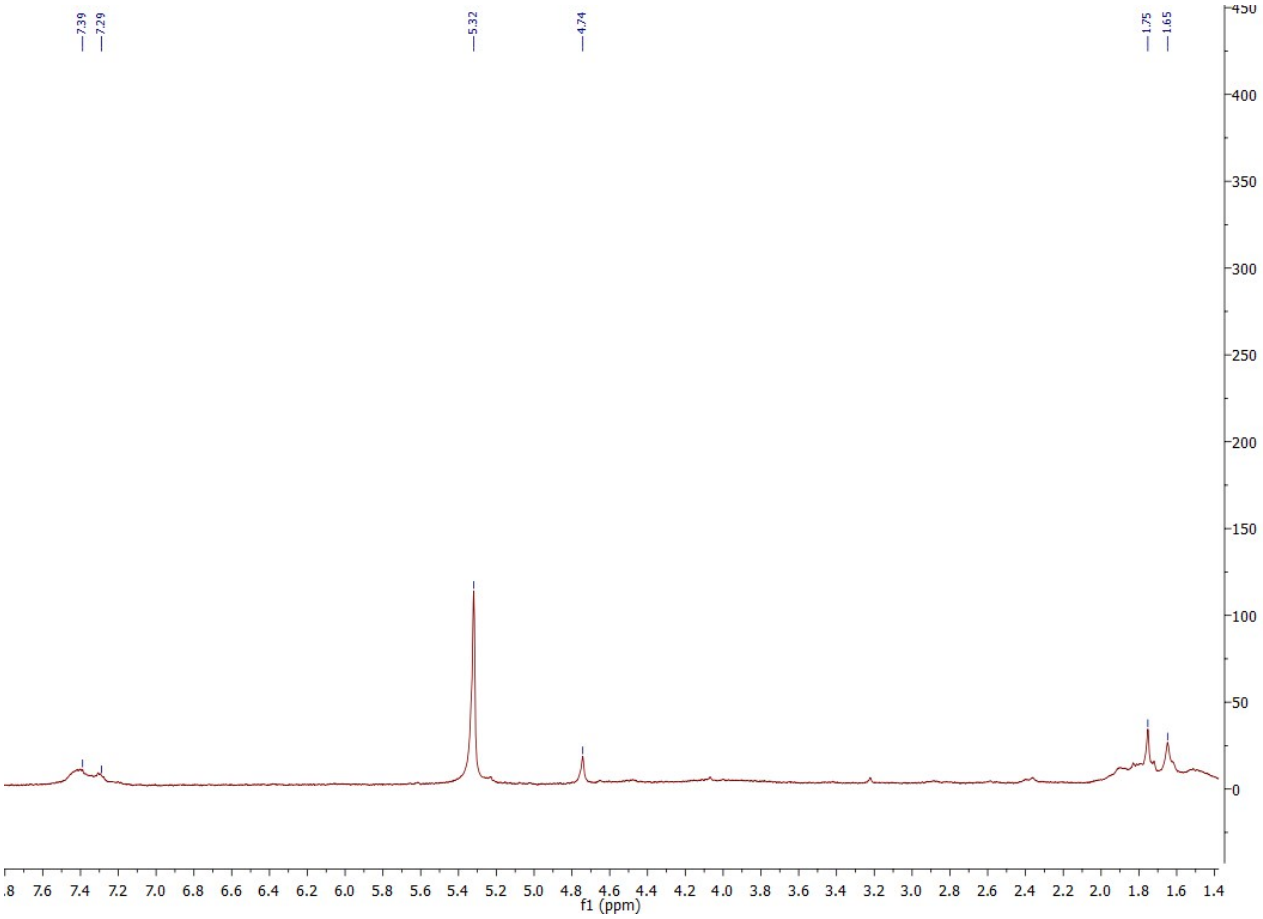

Figure S14: ^{1}H NMR spectrum of the complex **(6)** in DCM.

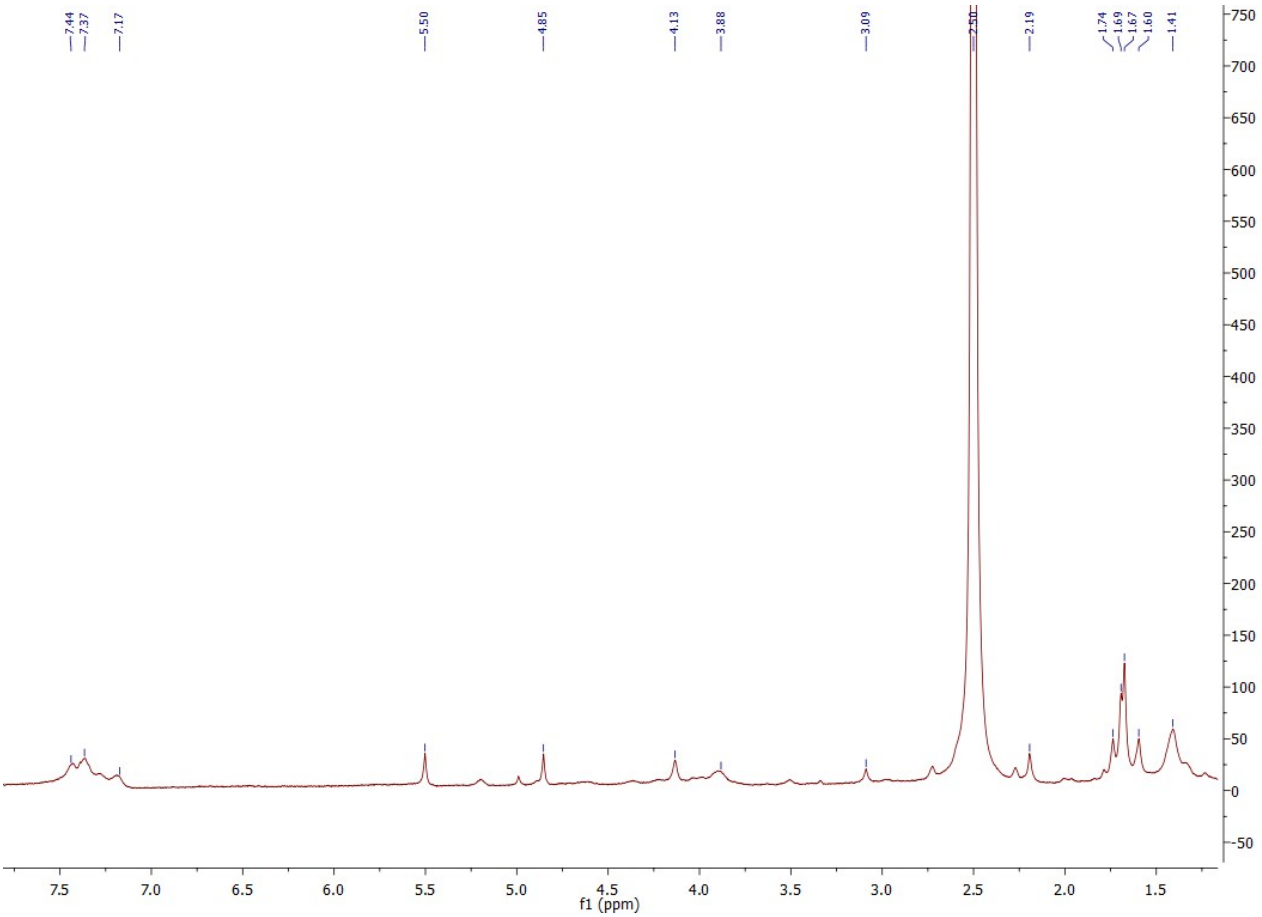

Figure S15: ^{1}H NMR spectrum of the complex **(6)** in DMSO.

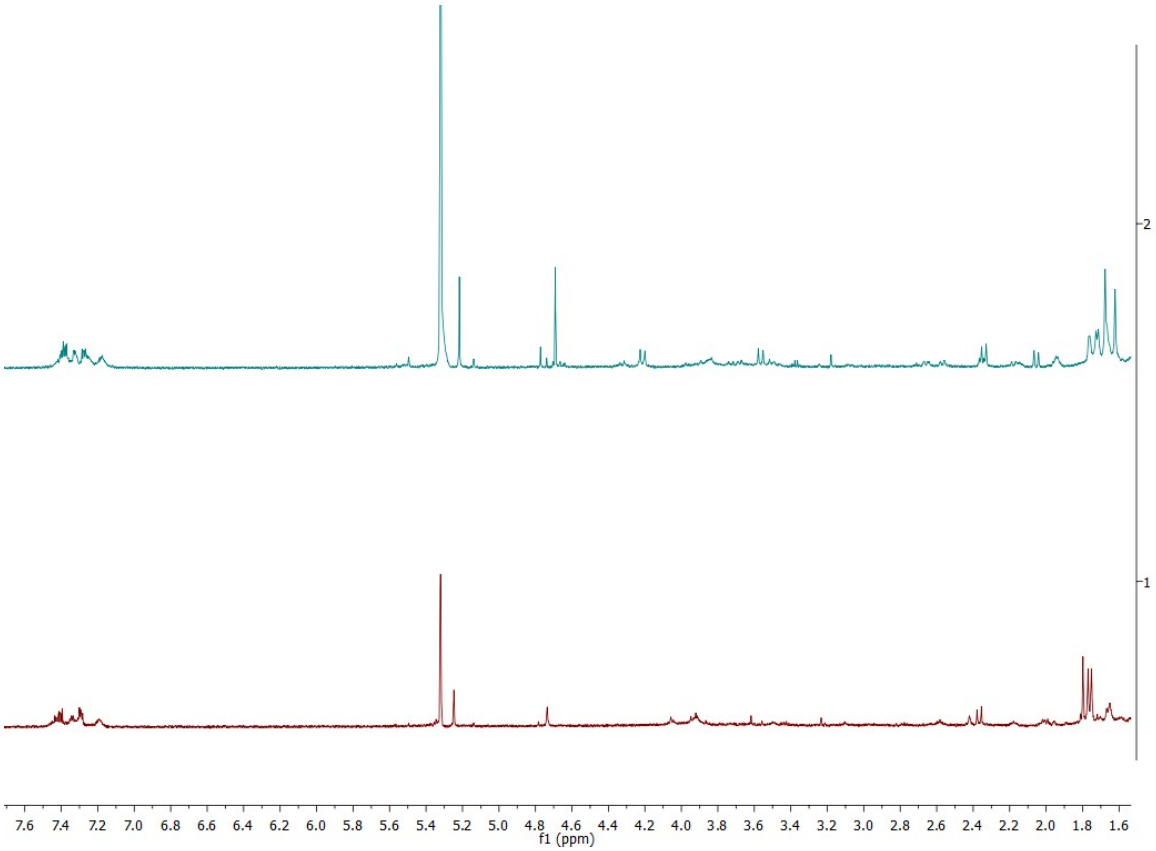

Figure S16: ^{1}H NMR spectrum of the complex **(6)** in DCM 214 K (top) and 296 K (bottom).

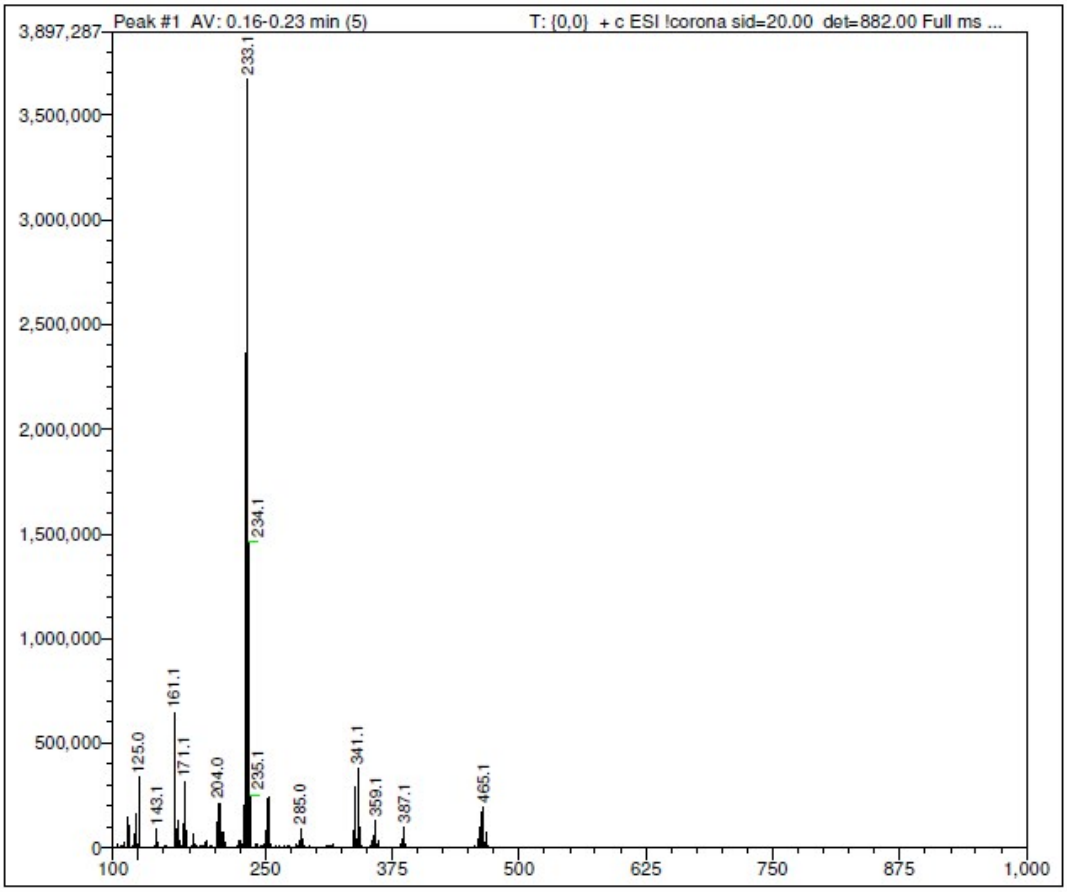

Figure S17: ESI-MS of ligand precursor **(1)** in H_2O: 233.1, calcd: 233.01 $[M-2Cl]^{2+}$.

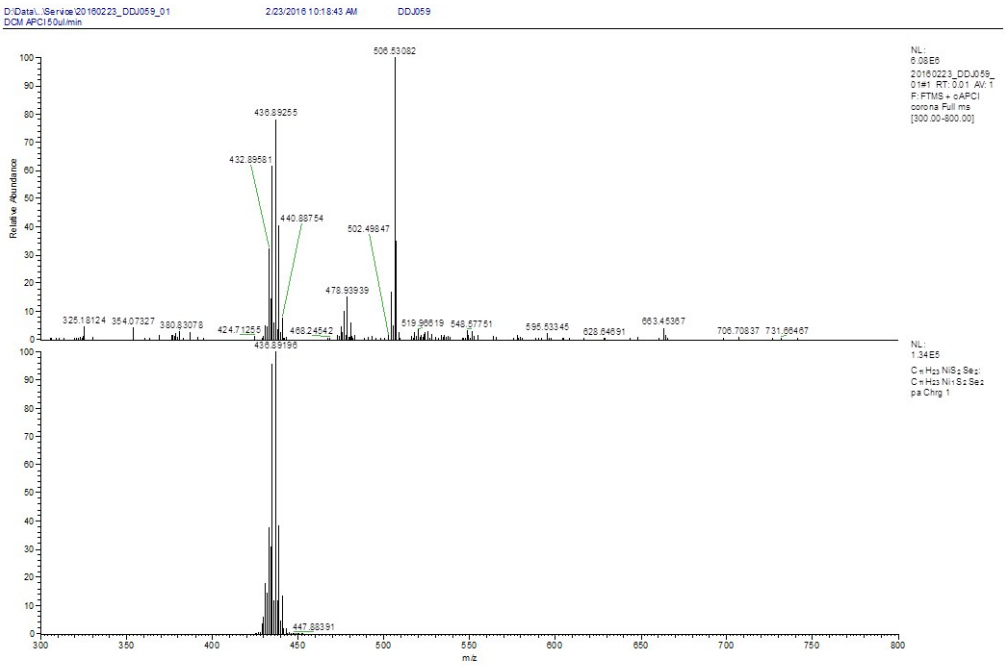

Figure S18: HR-MS of complex **(3)** in DCM: 436.89255, calcd: 436.89196 $[M+H]^+$ experimental spectrum (top) and simulated spectrum (bottom).

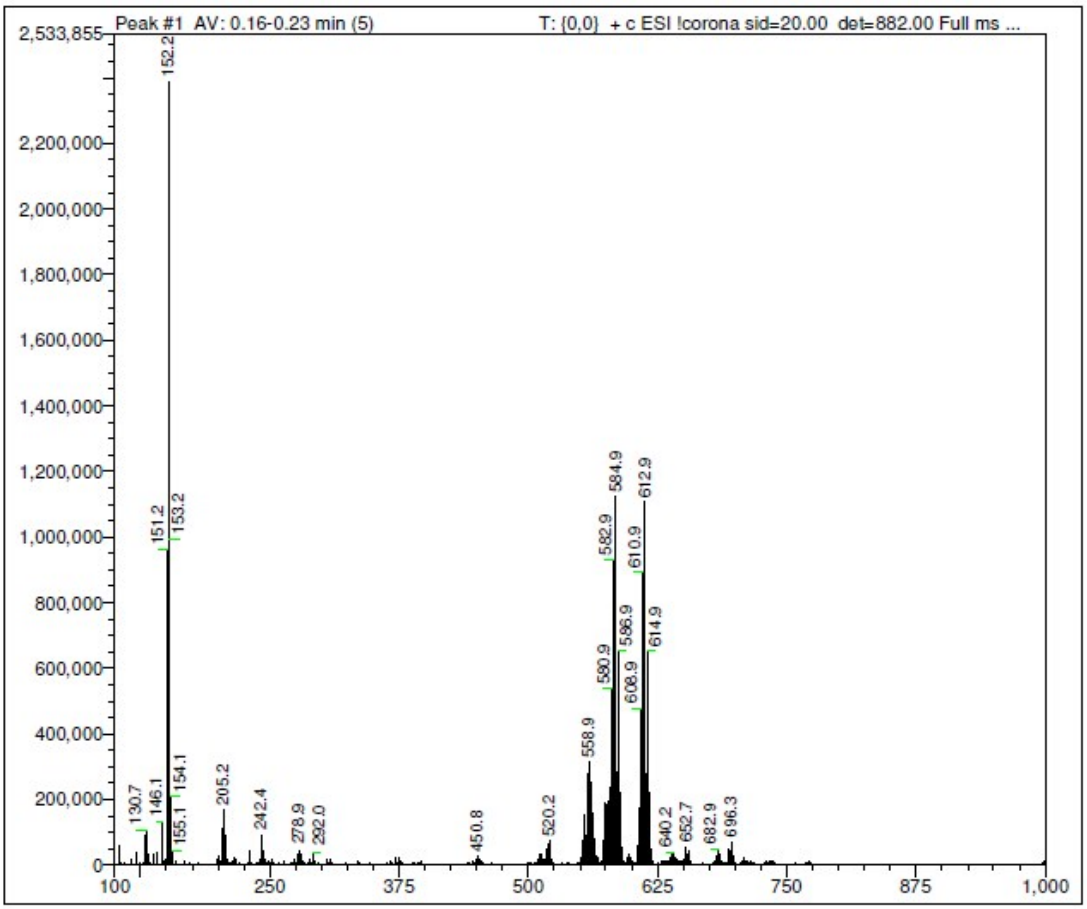

Figure S19: ESI-MS of complex **(5)** in MeCN: 584.9, calcd: 584.9 $[M-PF_6]^+$, 612.9, calcd: 612.9 $[M-(PF_6)+(CO)]^+$, 556.9, calcd: 556.9 $[M-(PF_6)-(CO)]^+$.

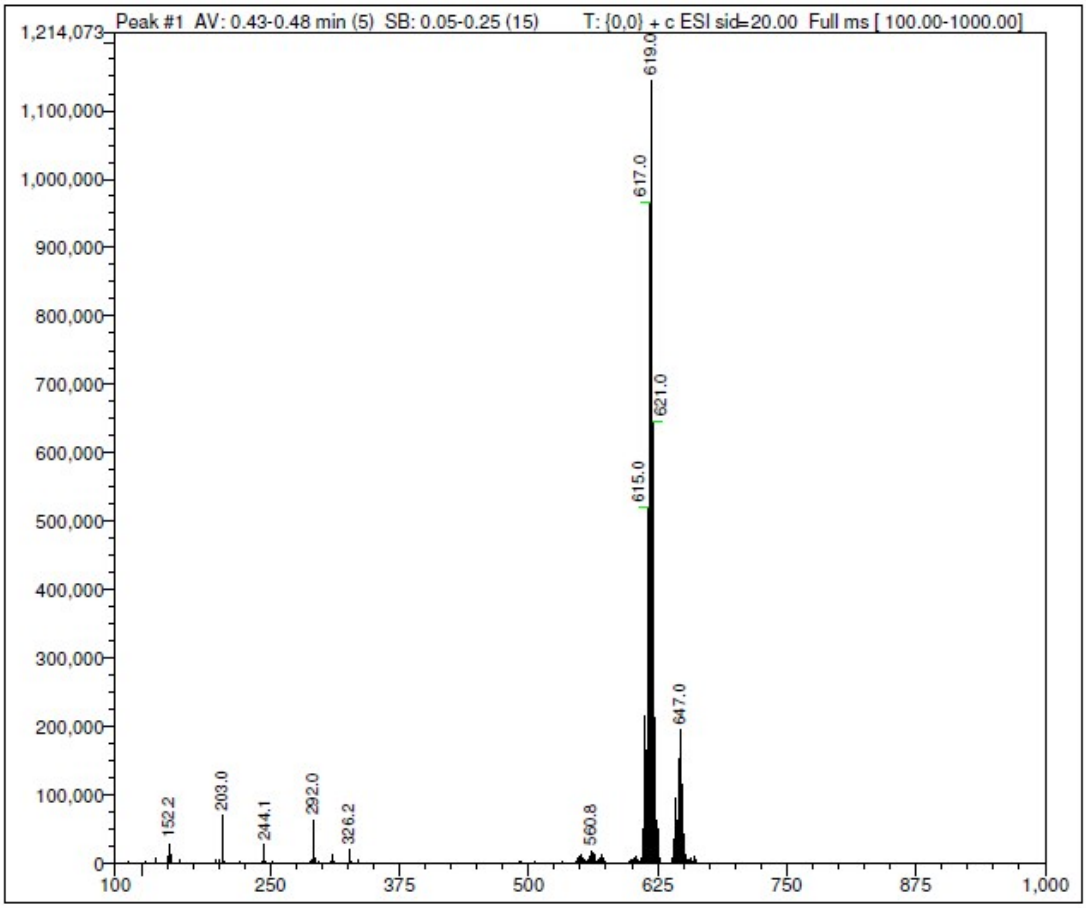

Figure S20: ESI-MS of complex **(6)** in MeCN: 619.0, calcd: 618.9 $[M-CO-PF_6]^+$, 647.0, calcd: 646.9 $[M-PF_6]^+$.

References

(1) Costentin, C.; Drouet, S.; Robert, M.; Savéant, J.M. *J. Am. Chem. Soc.* 2012, **134**, 11235.

(2) Elgrishi, N.; Chambers, M. B.; Fontecave, M. *Chemical Sci* 2015, **6**, 2522.